

Photovoltaic and diffusion effects in formation of 1D and 2D gratings by Bessel beam technique in $\text{LiNbO}_3\text{:Fe}$ crystal

Anahit Badalyan, Ruben Hovsepyan, Vahram Mekhitarian, Paytsar Mantashyan* and Rafael Drampyan

Institute for Physical Research, National Academy of Sciences of Armenia, 0203, Ashtarak-2, Republic of Armenia

ABSTRACT

The study of the contributions of photovoltaic and diffusion effects in the formation of 1D and 2D holographic gratings by Bessel beam technique in photorefractive Fe doped lithium niobate crystals are performed. For this purpose 1D and 2D gratings were recorded by travelling Bessel beam and counter-propagating Bessel beam (CPBB) techniques using laser radiation at 532nm wavelength and 17 mW power. Created 1D grating in the form of concentric rings had 9.0 μm period in radial direction. 2D grating which is a combination of annular and planar gratings had a period of 9.0 μm in radial and 266 nm in axial directions. The testing of the profile of the recorded gratings by phase microscope was performed. The investigations show that the refractive index depth of modulation for 1D annular grating has pronounced azimuthal dependence as a result of formation of gratings predominantly by the photovoltaic effect taking place along the C-axis of the crystal. For 2D grating formed by CPBB technique the azimuthal dependence of grating modulation depth is less pronounced. The 266 nm period in axial direction provides, except for the photovoltaic effect, also the contribution of the diffusion of charge carriers to the grating formation. Diffusion effect takes place in all directions and provides the isotropic contribution to the grating formation, but with less efficiency than the photovoltaic effect.

Keywords: holographic gratings, photorefractivity, photovoltaic and diffusion mechanism, lithium niobate, Bessel beam

1. INTRODUCTION

Among different methods for the fabrication of artificial periodic structures in dielectric materials the holographic technique¹ is one of the promising methods for fabrication of photonic lattices. Holographic technique is based on the creation of spatially periodical structures by intensity modulated light beams in photosensitive materials. There are two main elements which are important for holographic recording: the method of creation of intensity modulated light beams and finding of suitable recording materials. Numerous investigations are devoted to the study of dynamic and permanent optical refractive gratings using classic two-beam interference arrangement in atomic vapors², crystals^{3,4} and liquid crystals (see, for example, Ref. [5] and references therein). The doped photorefractive crystals are very convenient materials for holographic recording. The illumination of photorefractive medium by spatially modulated beam leads to the refractive index modulation via electro-optic effect, thus creating refractive gratings. The light excites the electrons from impurity ion state to conduction band. Electrons migrate in the conduction band and finally are trapped by ions. The redistribution of the charges builds up an internal electric field E and so changes the refractive index $\Delta n_i = r_{ij}E_j$, where r_{ij} is the electro-optic coefficient. The charge transport is mainly due to the photovoltaic and diffusion of charge carriers⁶⁻⁹. The relative contribution of photovoltaic and diffusion effect depends on the grating periods and crystal parameters and was a subject of studies, both experimental^{3,4,9} and theoretical⁷⁻⁹. Recently developed traveling Bessel beam technique for formation of 1D micrometric scale annular grating and counter-propagating Bessel beam (CPBB) technique for formation of 2D grating, which is the combination of micrometric scale annular grating and sub-micrometric scale planar grating (see Ref.[10]) are very convenient to study the relative contribution of photovoltaic and diffusion effects in grating formation. The additional modulation of 2D grating in axial direction with a period of 266 nm with the use of CPBB technique¹⁰ provides the additional contribution of diffusion effect in grating formation compared with micrometric scale 1D grating, which formed predominantly by photovoltaic effect.

In the presented experiment 1D and 2D refractive gratings were formed by Bessel beams technique¹⁰ in Fe doped lithium niobate (LN:Fe) crystal. The testing of the recorded gratings by phase microscope was performed, which allowed to

*paytsar.mantashyan@gmail.com

reveal the contribution of two main mechanisms – photovoltaic and diffusion effects in formation of 1D and 2D gratings in the photorefractive LN:Fe crystal taking into account the periods of the gratings and crystal parameters.

2. EXPERIMENT

2.1 Recording of 1D and 2D gratings by Bessel beams technique

1D and 2D refractive gratings were recorded by traveling Bessel beam and CPBB techniques to study the contributions of photovoltaic and diffusion mechanisms in formation holographic gratings in photorefractive LN:Fe crystals.

Bessel beams or diffraction-free beams are a specific type of coherent beams¹¹. Bessel beams have a feature of conserving their transverse intensity distribution, expressed by the zeroth-order Bessel function, while they propagate in free space. The simplest diffraction-free beams can be formed by superposition of plane waves whose wave vectors lie on the cone. One of the ways for creation of Bessel beams is the use an optical element- axicon¹². The scheme for the Bessel beam formation from Gaussian 633 nm beam by an axicon is shown in Figure 1a. The convergence angle of the beams passed through the axicon was adjusted by moving the output lens of the beam expander back or forth, thus varying the convergence angle within $\sim 3\text{-}4^\circ$, which, in turn, changes the spacing between the concentric rings in the range of 10 - 25 μm . Ideal Bessel beam has no intensity gradient along the propagation axis and can be schematically represented as a set of co-axial hollow light cylinders surrounding the central light rod. The profile of Bessel beam is a set of concentric rings (Figure 1b). Bessel beam becomes divergent behind the overlapping zone and form a ring pattern in the far field (Figure 1a).

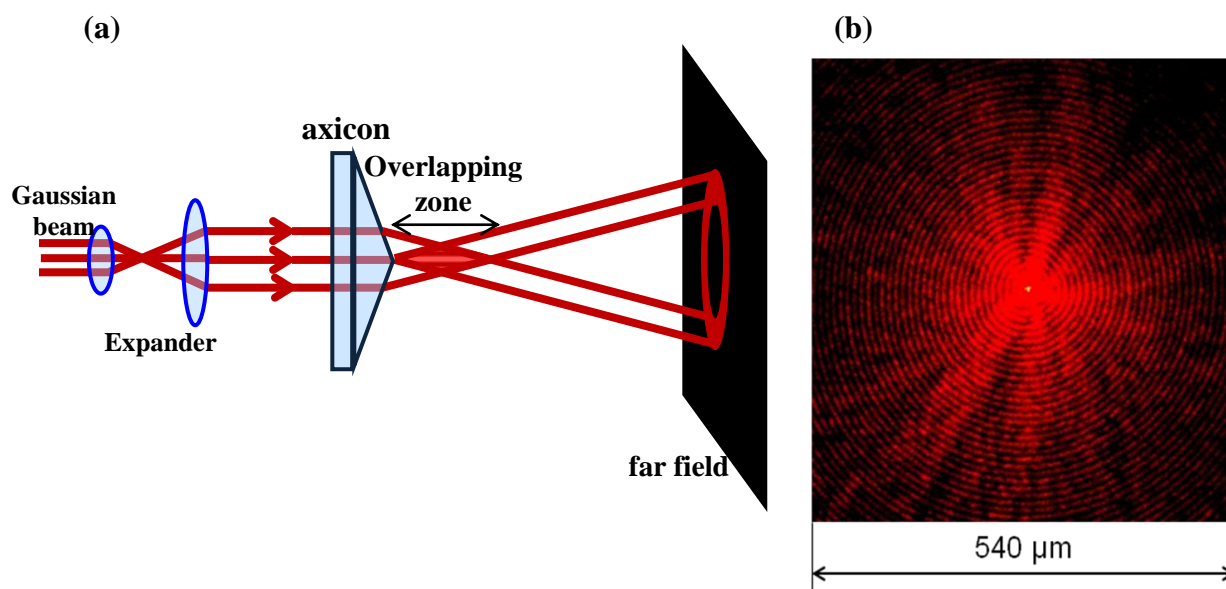


Figure 1. (color online). (a) Experimental scheme illustrating the formation of Bessel beam by axicon. (b) Fragment of radial intensity distribution of Bessel beam formed by axicon with aperture cone angle 175° in the overlapping zone of the beams. The spacing between the concentric rings, measured by beam profiler, shows their equidistant disposition, except for few central rings. The period of annular structure shown in the figure equals $\sim 10\text{ }\mu\text{m}$ for certain position of output lens of the beam expander. The number of rings reaches up to 1000.

The annular ring pattern is two-dimensional, however, as an annular grating this structure is one-dimensional with the period determined by the spacing between rings. However, the intensity modulation along Z axis can be obtained by creating the Bessel standing wave in CPBB geometry.

The experimental scheme of recording of 2D gratings by CPBB technique is shown in Figure 2. The laser source was single-mode second harmonic of cw YAG:Nd laser at 532 nm wavelength with linear polarization and 100 mW

maximum power. The recording of grating was performed by laser beam power 17 mW. The laser beam was expanded by confocal lenses and after passing through the axicon with 175° aperture cone angle was transformed into the Bessel beam. LN crystal doped by 0.05 wt% Fe was placed in the overlapping zone of the beams after axicon. The beam intensity in the lattice recording area is estimated $\sim 47 \text{ mW/cm}^2$. Optical C-axis of the crystal was oriented along the crystal surfaces. The dimensions of the crystal were $15\text{mm} \times 10\text{mm} \times 2\text{mm}$. The back-reflecting mirror was situated 1 cm far from the crystal. 1D annular grating was recorded simply removing the back reflecting mirror shown in Figure 2.

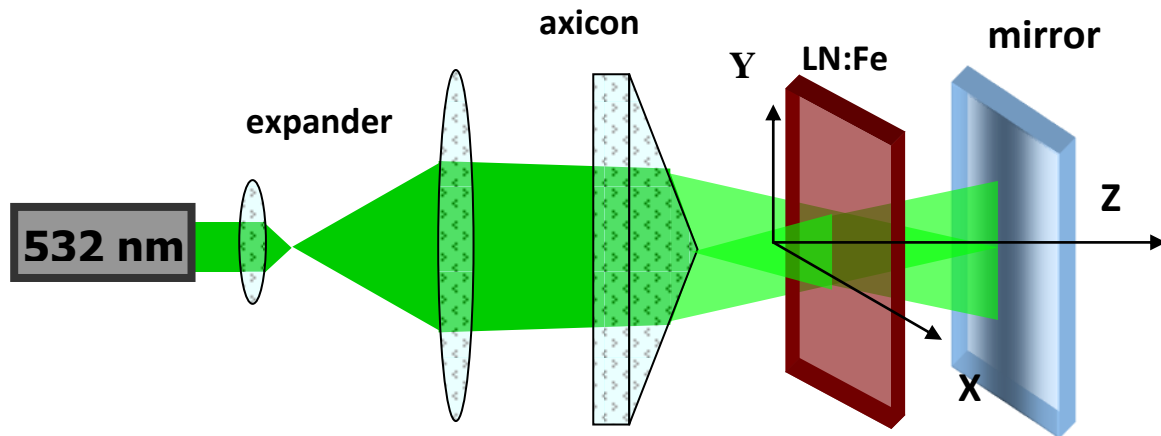


Figure 2 (color online). Schematic for creation of 2D grating by single axicon and back-reflecting mirror. Ideal Bessel beam has no intensity gradient along the propagation axis. However, the intensity modulation along Z axis can be obtained by creating the Bessel standing wave in counter-propagating Bessel beam geometry. Optical C-axis of the crystal is directed along the Y axis.

The recording of gratings was performed during 60min illumination. Recorded 1D grating is the annular structure with period in radial direction measured of $9.0\mu\text{m}$. The formed 2D structure is a combination of annular and planar gratings with $9.0\mu\text{m}$ period in radial direction and half-wave period (266 nm) in axial direction. Fragment of 2D structure schematically is shown in Figure 3. The diffraction-free character of Bessel beams provides the creation of high contrast volume gratings.

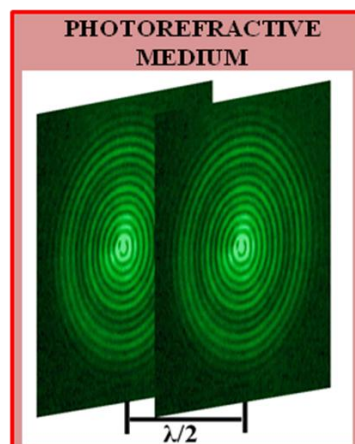


Figure 3. (color online). Schematic of two neighboring planes of standing wave with maxima of light intensities, separated by half wavelength $\lambda/2$, where the concentric rings are located.

2.2 Testing of recorded gratings

The recorded gratings were tested using red laser beam with 4mW power by observing the diffraction patterns from the gratings in the far field. Figure 4 shows the readout scheme for testing of gratings recorded inside the crystal. The testing was performed by red beam to avoid the erasure of the grating during readout⁴.

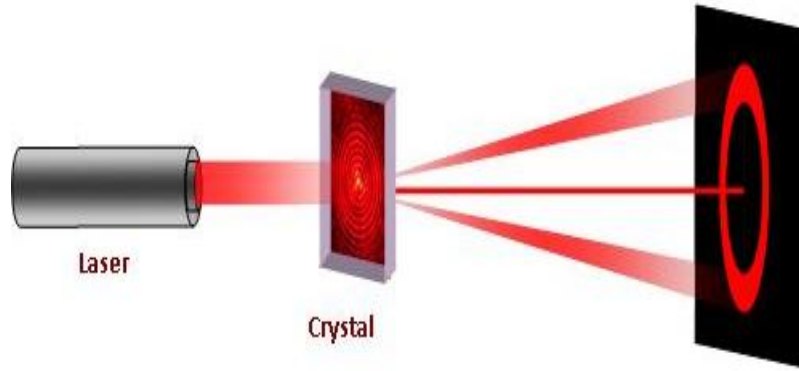


Figure 4. (color online). Readout scheme for testing by red laser of gratings recorded by green laser. The screen situated in the far field shows the hypothetical diffraction pattern.

Figure 5a shows the result of testing by Gaussian beam of 2D grating recorded in Y-cut LN:Fe. The far field transmitted diffraction pattern (Figure 5a) consists of two opposite disposed segments of a ring. Figure 5(b) shows the transmitted beam pattern from the “clean” part of the crystal without recorded grating.

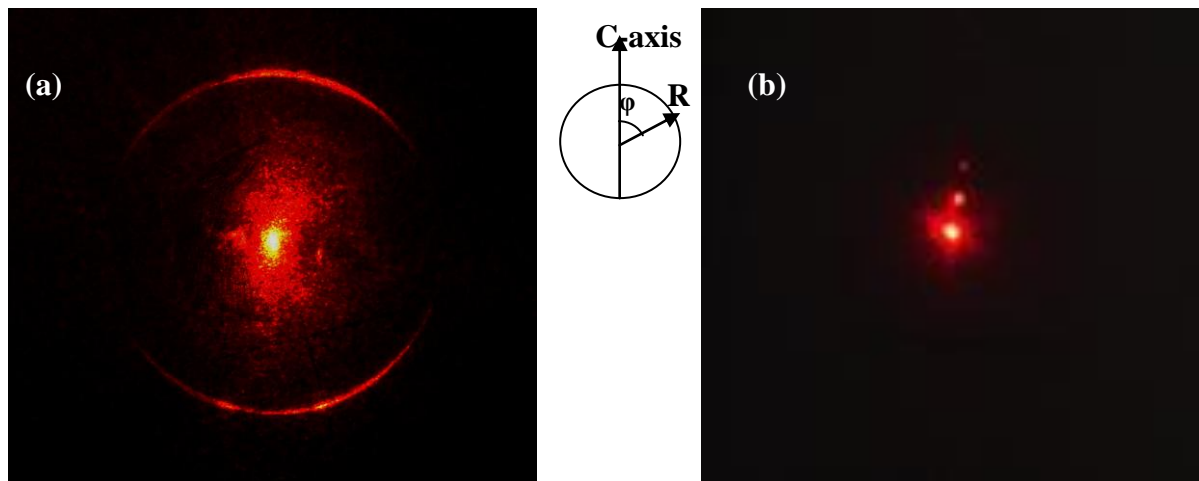


Figure 5. (color online). (a) Far field transmitted diffraction pattern from 2D refractive grating, recorded in Y-cut LN:Fe during 60 min, for nearly orthogonal incidence of the probe Gaussian beam at 633 nm to the crystal surface. Solid arrow shows the direction of C-axis of the crystal relative to the diffraction pattern. (b) Transmitted beam pattern from the “clean” part of the crystal without recorded grating. The bright spots correspond to the multiple reflections of beam from the surfaces of the crystal.

The diffraction pattern from 1D and 2D grating has pronounced azimuthal dependence of intensity distribution with higher diffracted intensity along the C- axis of the crystal. No essential difference in diffraction from 1D and 2D gratings was observed for orthogonal incidence of probe beam to the crystal surface. To understand the azimuthal dependence of diffraction pattern and to investigate the different contributions of photovoltaic effect and diffusion of charge carriers in formation of 1D and 2D gratings in LN:Fe crystal by Bessel beam technique, the direct observation of 1D and 2D

periodic structures was performed by phase microscope. The profiles of recorded 1D and 2D gratings are shown in Figure 6 a, c, respectively.

The dashed white lines mark the areas where the grating is recorded with high contrast (right and left sectors) and does not recorded at all (upper and lower sectors) in the case of 1D grating.

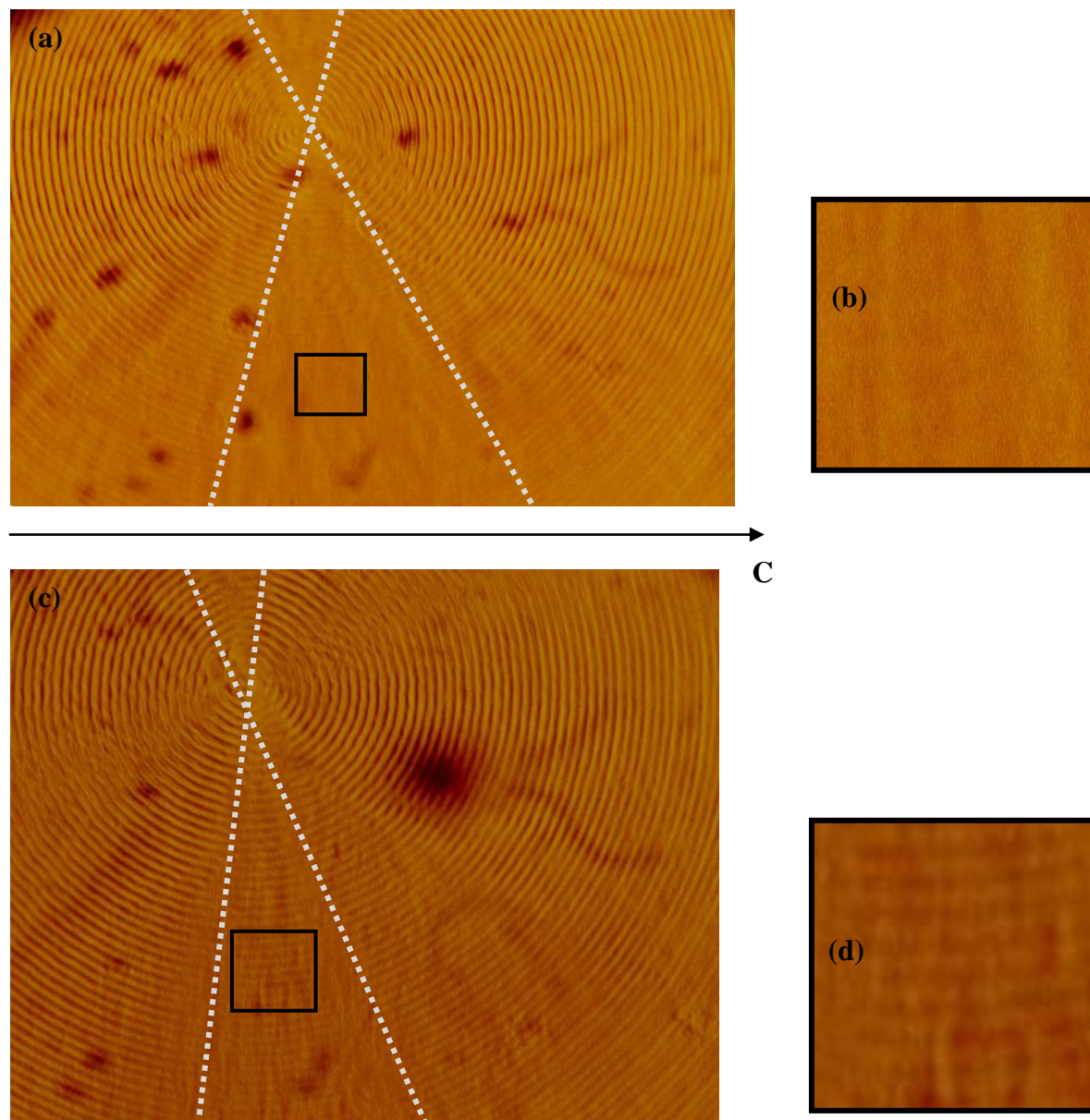


Figure 6 (color online). Fragments of phase microscope images of 1D (a) and 2D (b) gratings recorded in LN:Fe crystals by traveling Bessel beam and standing Bessel beam techniques, respectively. The solid arrow shows the direction of optical C-axis of the crystal. The dashed white lines mark the areas where the gratings are recorded with high contrast (right and left sectors on (a) and (c)) and does not recorded at all (upper and lower sectors in the case of 1D grating on (a)). (b) and (d) are enlarged patterns of regions, marked by solid black rectangles.

In the case of 2D grating the ring pattern appears in the regions (Figure 6 c,d) where no grating was recorded in the case of 1D grating (Figure 6b), however, with less contrast. The difference between phase microscope images of profiles for

1D and 2D gratings is due to different contribution of two main mechanisms – photovoltaic and diffusion effects in formation of 1D and 2D gratings inside the photorefractive crystal.

3. DISCUSSION

The physical mechanism of formation of holographic grating in photorefractive materials is based on the electro-optic effect. Fe ions occur in LN crystal in different valence states: Fe^{2+} and Fe^{3+} . The corresponding band diagram is shown in Figure 7. The green light excites the electrons from Fe^{2+} to conduction band. Electrons migrate in the conduction band and finally are trapped by Fe^{3+} . The redistribution of the charges builds up an internal space charge electric field E and so changes the refractive index Δn . Thus, the inhomogeneous illumination of photorefractive materials leads to the modulation of refractive index.

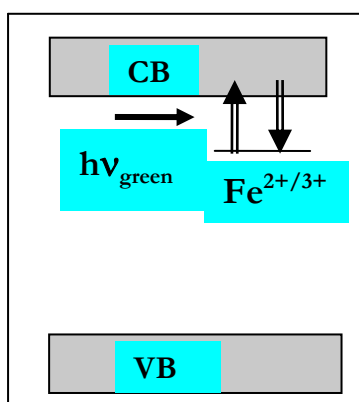


Figure 7. Band diagram of lithium niobate doped with iron. CB is the conduction band, VB is the valence band.

In Fe doped LN crystal the change of extraordinary refractive index is larger than the change of ordinary index by a factor of four¹¹ and the induced refractive index change δn is mainly due to the distortion of extraordinary index of refraction. The main mechanisms for electric field induction in the crystal are spatial charge separation caused by photovoltaic effect, taking place along the C-axis of the crystal, and diffusion of the charge carriers^{7,8,13}. Induced electric field E along C- axis of the crystal is determined by⁸

$$E(Y) = E_{PV} + E_{dif} = \alpha k I / \sigma + (e D_e / \sigma) dn_e / dY \quad (1)$$

where E_{PV} and E_{dif} are the internal electric fields due to photovoltaic effect and charge diffusion, respectively, α is the absorption coefficient, k is the Glass constant depending on the nature of absorbing centers and light wavelength, I is the light intensity, σ is the conductivity of the illuminated part of the crystal, e is the electron charge, D is the diffusion coefficient, n_e is the concentration of photo-excited charge carriers. In formula (1) Y coordinate is considered to be directed along C-axis of the crystal. The electric field induced in the crystal along the axial direction (Z -axis in Fig 2) is determined by diffusion effect.

As shown in Ref. [8] for Fe doped LN crystal the diffusion effect for charge carriers can be neglected for grating spatial frequencies $K = 1/d$ having the values less than $\sim 10^3$ lines/cm, where d is the grating period.

For 1D gratings recorded by traveling Bessel beams the diffusion effects of charge carriers are negligible because the grating period $d = 9.0 \mu\text{m}$ corresponds to the spatial frequency $K \sim 10^3$ lines/cm and photovoltaic mechanism taking place along the C-axis is the predominant process. The azimuthal dependence of the contrast of the recorded grating can be explained qualitatively by following consideration. The distance between bright and dark zones in the central part and on the periphery of the Bessel beam profile along the C axis of the crystal is essentially different. So the probability of the migration of electrons from bright to dark zone and final trapping of the electrons in dark zone is higher in the central region compared with the periphery. As a consequence the azimuthal dependence of the modulation depth of the

recorded grating appears which is clearly demonstrated by azimuthal dependence of the contrast of phase microscope image of the grating shown in Figure 6a. However, additional studies, both experimental and theoretical, are required to confirm the suggested model. In particular, the recording of the gratings at higher intensities, as well as for different concentrations of impurity ions are planned to be performed.

For 2D grating formed by CPBB technique the half-wave 266 nm period in axial direction corresponds to the spatial frequency $K \sim 4 \times 10^4$ lines/cm and the diffusion effect taking place in all directions also contributed to the grating formation but with less efficiency than photovoltaic effect. This is illustrated by phase microscope image in Figure 6d.

4. CONCLUSION

1D and 2D refractive gratings were created by Bessel beams technique in photorefractive LN:Fe crystals. The testing of the gratings by phase microscope shows that for 1D gratings with 9.0 μm period in radial direction the diffusion effect can be neglected and the photovoltaic effect is the predominant process for formation of gratings. This in turn leads to azimuthal dependence of the contrast of the annular grating. For 2D grating, which is the combination of annular and planar gratings, the 266 nm period in axial direction provides the contribution of diffusion effect but with less efficiency compared with photovoltaic effect.

ACKNOWLEDGEMENTS

The authors are grateful to Dr. E Kokanyan for providing the LN:Fe crystal. This work was supported by International Science and Technology Center Grant, Project A-1517.

REFERENCES

- [1] Collier R. J., Buckhard Ch. B., Lin L. H., [Optical holography], Academic press, New York, 1971.
- [2] Korneev N., Benavides O., "Mechanisms of holographic recording in rubidium vapor close to resonance", JOSA B, 25, 1899 – 1906 (2008).
- [3] "Photorefractive materials, effects and devices. Control of light and matter", Applied Physics B, special issue, V. 95, N.3 (2009).
- [4] Adibi A., Buse K., Psaltis D., "Two-center holographic recording", JOSA B, 18, 584-601 (2001).
- [5] Pagliusi P., Macdonald R., Bush S., Chipparrone G., Kreuzer M., "Nonlocal dynamic gratings and energy transfer by optical two-beam coupling in a nematic liquid crystal owing to highly sensitive photoelectric reorientation", JOSA B, 18, 1632-1638 (2001).
- [6] Adibi A., Buse K., Psaltis D., "The role of carrier mobility in holographic recording in LiNbO_3 ", Appl. Phys. B 72, 653–659 (2001)
- [7] Chen F. S., "Optically induced change of refractive indices in LiNbO_3 and LiTaO_3 ", J. Appl. Phys. 40, 3389-3396 (1969).
- [8] Glass A. M., D. von der Linde, Negran T. J., "High-voltage bulk photovoltaic effect and the photorefractive process in LiNbO_3 ", Appl. Phys. Lett. 25, 233-235 (1974).
- [9] Avanesyan G. T., Vartanyan E. S., Mikaelyan R. S., Hovsepyan R. K., Pogosyan A. R., "Mechanisms of photochromic and photorefractive effects in doubly doped lithium niobate crystal", Phys.Stat.Sol. (a) 126, 245 – 252 (1991).
- [10] Badalyan A., Hovsepyan R., Mekhitarayan V., Mantashyan P., Drampyan R., "New holographic method for formation of 2D gratings in photorefractive materials by Bessel standing wave" in "Fundamentals of Laser Assisted Micro- and Nanotechnologies 2010, edited by Vadim P.Veiko, Tigran A. Vartanyan, Proceedings of SPIE, Vol. 7996 (SPIE Bellingham, WA, 2011) 799611-1-9.J.
- [11] Durnin, Mikely J. J., Jr, Eberly J. H., "Diffraction-free beams", Phys. Rev. Lett. 58, 1499-1501 (1987).
- [12] Shafer F. P., "On some properties of axicons", Appl. Phys. B, 39, 1-8 (1986).
- [13] Johansen P.M. "Linear and Nonlinear Space-Charge Field Effects in Photorefractive Materials", Risø National Laboratory, Roskilde(2001)